Oct 20th, 12:00 AM

Local and Distortional Buckling of Thin-walled Beams

Reynaud Serrette

Teoman Pekoz

Eleventh International Specialty Conference on Cold-Formed Steel Structures
St. Louis, Missouri, U.S.A., October 20-21, 1992

LOCAL AND DISTORTIONAL BUCKLING OF THIN-WALLED BEAMS

Reynaud Serrette[1] and Teoman Pekőz[2]

Summary

Recent research has characterized the behavior of panel beams with laterally unsupported compression flanges as either a complex local buckling mode or an overall buckling mode. Tests have shown that the behavior of the unsupported flange and web is similar to that of lateral buckling, except, rotation is enforced along the axis of the web and the tension flange--a behavior which may be described as distortional buckling. In the work described here, an analytical expression is presented for computing the elastic distortional buckling stress based on a model which treats the web and compression flange as an elastically restrained beam. The formulation is similar to those for lateral and torsional buckling. The effect of web local buckling on the rotational restraint of the outstanding leg is modeled explicitly using the effective width equations described in the AISI Cold-Formed Steel Design Manual. The analytical results from the distortional buckling expression are shown to agree reasonably well with numerical results generated from an elastic finite strip buckling program (BFINST6). A design approach is suggested for estimating the ultimate moment capacity of a section subjected to the interaction between local and distortional buckling.

Introduction

The distortional buckling behavior of the unsupported compression flange and web in panel beams is similar to that of lateral buckling. However, for distortional buckling, rotation of the web-flange element is enforced along the axis of the web and the tension flange, as illustrated in Figure 1. This behavior has been referred to in earlier studies as local lateral buckling.

Recommendations for the design of flexural members are given in various specifications for local, distortional and lateral buckling, and for local-lateral buckling interaction (AISI, 1986; EC 3, 1989). Of the available design guidelines, only the AISI Specification considers the distortional buckling mode described here. This specification does not, however, provide explicit design guidelines for the interaction between local and distortional buckling. In addition, the present AISI design rules were shown to be overly conservative for panels similar to those currently used in industry (Cohen, 1987).

In the work described here, an analytical expression is presented for computing the elastic distortional buckling stress based on a model which treats the web and compression flange (outstanding leg) as an elastically restrained beam. The derived expression is similar in form to the expression for lateral buckling. The effect of web local buckling on the rotational restraint of the outstanding leg is modeled explicitly using the effective width equations described in the AISI Cold-Formed Steel Design Manual. The predicted elastic behavior from the analytical model is found to compare well with the results from an elastic finite strip buckling analysis and the interaction between local and distortional buckling is treated in a model which assumes that distortional buckling occurs before local buckling.

Experimental Studies

Douty (1959-62) conducted an extensive test program (fifty-seven specimens) on the behavior of channel and inverted hat sections subjected to flexure. The nominal dimensions and yield strength of the specimens included in Douty's study are given in Table 1. For the overall loading scheme shown in Figure 2, Douty noted both local-distortional and local-lateral buckling interactions in his specimens. However, local-distortional buckling interaction was the governing mode of failure for the majority of specimens. Local-lateral buckling interaction was prevalent in sections with narrow tension flanges.

[1] Asst. Professor, Department of Civil Engineering, Santa Clara University, Santa Clara, CA 95053
[2] Professor, School of Civil and Environmental Engineering, Cornell University, Ithaca, NY 14853

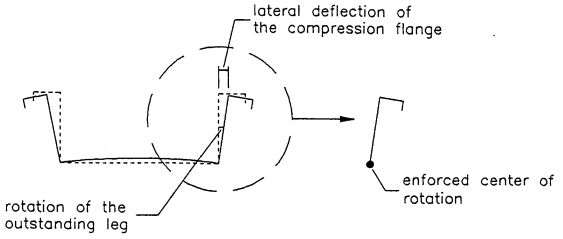

Figure 1 Distortional buckling behavior

Table 1 Properties of the sections tested by Douty

Specimen	w1 in.	w2 in.	w3 in.	w4 in.	t in.	F_y ksi
S1-XB*	0.00	1.50	3.00	3.50	0.11	40.0
S2-AX*	"	"	6.00	"	"	41.2
S2-XB*	"	"	"	"	"	"
S3-AX**	"	1.25	4.00	8.00	"	40.0
S3-XB**	"	"	"	"	"	"
S4-XB**	"	"	8.00	8.00	"	40.5
S5-XB-A*	0.75	1.75	4.50	12.0	"	38.7
S5-XB-B*	"	"	"	"	0.06	44.0
S6-XB-A*	"	"	7.50	"	0.11	36.5
S6-XB-B*	"	"	"	"	0.06	45.0
PS-X**	0.50	0.87	2.87	16.0	0.03	38.0

* inverted hat section; ** channel section

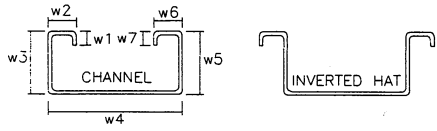

To augment Douty's test results, a recent test program was undertaken at Cornell University. These tests included panel geometries which are currently produced by U.S. manufacturers. The primary modifications to Douty's panel dimensions included the thickness, symmetry of the section, and the configuration of the compression flange edge stiffener. The nominal dimensions of the sections used in the study are given in Table 2 and a symmetric two-point loading scheme similar to Douty's was used.

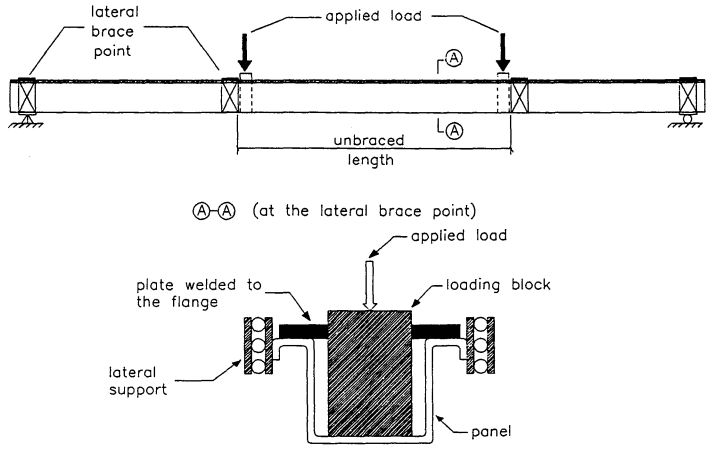

Figure 2 Douty's test setup

Table 2 Properties of the sections tested in the recent Cornell study

Specimen	w1 in.	w2 in.	w3 in.	w4 in.	w5 in.	w6 in.	w7 in.	w8 in.	θ deg.	t in.	F_y ksi
DNL33*	0.00	1.00	3.00	3.00	---------	SYMMETRIC	----------		0.00	0.02	58.0
DL33*	0.50	"	"	"		"			"	"	"
DNL55*	0.00	"	5.00	5.00		"			"	"	"
DL55*	0.50	"	"	"		"			"	"	"
TEST 1-3#	0.31	0.68	1.93	15.94	2.00	0.78	0.65	0.20	20.0	"	"
TEST 4#	"	"	"	"	"	0.67	0.00	0.00	0.00	"	"
TEST 5#	"	"	"	"	"	0.78	0.28	0.00	20.0	"	"

* inverted hat section; # non-symmetric section

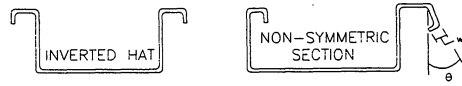

Behavior similar to that described by Douty--interaction between distortional buckling and local buckling in the webs, flanges and lips--was observed in all the tests. Figure 3 shows the typical mode of failure for the specimens in the current tests. The displacement of the outstanding leg was described by a lateral deflection of the compression flange and the formation of a "local mechanism" at the web-compression flange junction of the outstanding leg (as indicated by the arrow).

Analytical Model

As mentioned earlier, distortional buckling may be described as a constrained lateral buckling of the outstanding leg. For the elastic problem, these constraints may be modeled as rotational and extensional springs located at the web-tension flange junction. Using the model shown in Figure 4, an expression for the distortional buckling stress of a section with laterally unsupported compression flanges was derived using classical bifurcation theory. In this model, no lateral displacement is allowed at the web-tension flange junction because the section as a whole is assumed to be laterally stable. Assuming plane sections remain plane, pure bending and simple supports, the elastic distortional buckling moment, $M_{cr,d}$, is given as

$$M_{cr,d} = \frac{\alpha_1 + \alpha_2}{\alpha_3} \qquad [1]$$

where $\alpha_1 = (EI_{xy}\eta\theta^2 + k_y\xi)^2$

$$\alpha_2 = -(EI_x\theta^2 + k_y)(EC_w\theta^2 + EI_y\eta^2\theta^2 + GJ\theta + K_y\xi^2 + k_\phi)$$

$$\alpha_3 = -(2\eta + \beta_1)(EI_x\theta^2 + k_y)\theta$$

$$\eta = y_o - h_y$$

$$\xi = x_o - h_x$$

$$\theta = \frac{\pi^2}{L_e^2}$$

E = Young's modulus
G = Shear modulus
I_x = moment of inertia about an axis normal to the web
I_y = moment of inertia about an axis parallel to the web
I_{xy} = product of inertia
β_1 = geometric parameter [= $1/I_x(\int_A y^3\,Da + \int_A x^2y\,Da) - 2y_o$]
C_w = warping constant
J = torsion constant
k_y = linear elastic extensional spring constant
k_ϕ = linear elastic rotational spring constant
(x_o, y_o) = coordinates of the shear center w.r.t. the centroid
(h_x, h_y) = coordinates of the web-tension flange junction w.r.t. the centroid
L_e = equivalent unsupported length of the leg

Preliminary studies and a consideration of the small difference in the moment of inertia of the outstanding panel legs indicated that the linear elastic extensional spring constant, k_y, may be approximated to zero for panels typically used in industry. The linear elastic rotational restraint constant, k_ϕ, was found to depend on the distortional buckling mode and the local buckling capacity of the web. For symmetric (s) and non-symmetric (as) buckling modes (see Figure 5), in sections with a width-to-thickness ratio of the tension flange less than 400 (see Figures 5(a) and 5(b)), the rotational spring constants may be taken, respectively, as

$$k_{\phi,s} = \frac{Et^3}{(1 - \nu^2)(6w_f + 4w_w)}\gamma \qquad [2]$$

and

$$k_{\phi,as} = \frac{Et^3}{(1 - \nu^2)(2w_f + 4w_w)}\gamma \qquad [3]$$

where t = thickness of the section
ν = Poisson's ratio
w_f = width of the tension flange
w_w = depth of the web in the leg under consideration
γ = ratio of the elastic local buckling stress in the web to the buckling stress required for the web to be fully effective (according to the AISI (1986) Specification for the Design of Cold-Formed Steel Structures)

Figure 3 Failure mechanism at the web-compression flange junction

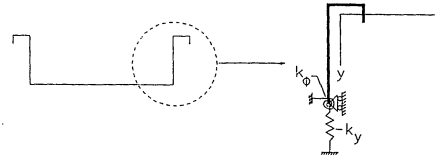

Figure 4 New model for distortional buckling

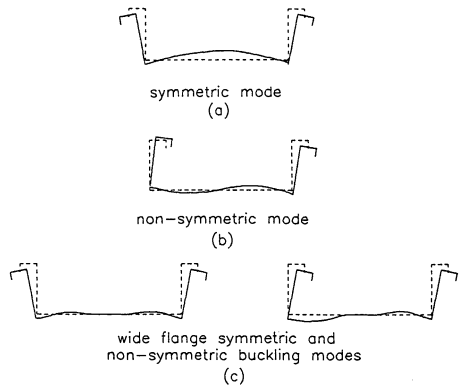

Figure 5 Symmetric and non-symmetric buckling modes

If the tension flange width-to-thickness limit is exceeded, then for the displaced shapes shown in Figure 5(c), parametric studies indicated that the rotational spring constants for the symmetric and non-symmetric modes are approximately equal and may be estimated by the expression

$$k_{\phi,s-as} = \frac{Et^3}{(1-\nu^2)\left(\frac{3}{4}w_f + 4w_w\right)}\gamma \qquad [4]$$

Comparison of Numerical and Analytical Results

Typical first and second mode buckling stresses derived from the elastic buckling finite strip program, BFINST6 (1978), are given by the curves labelled numerical in Figures 6 and 7, for the PS-X specimen from Douty's tests and test 1-3 from the recent Cornell study. These buckling curves show the relationship between the elastic buckling stress and the half-wavelength (unsupported length of the compression flange) assuming a single buckled half sine wave. The distorted shapes associated with the numerical curves, show that distortional buckling occurs at intermediate half-wavelengths between those for local and lateral buckling.

A comparison of the analytical buckling curves with the numerical curves in Figure 6, shows that:

- *the minimum numerical local buckling stress is bounded by the analytical (AISI, 1986) flange and web local buckling stresses*
- *the analytical distortional buckling curve agrees well with the portion of the numerical curve which describes distortional buckling*
- *the numerical and analytical curves show good agreement for half-wavelength which characterize lateral buckling*

In addition, point B on the numerical curve shows that if distortional buckling and local buckling occur at the same half-wavelength, the capacity of the section can be greatly reduced. The discrepancy between the analytical and numerical curves in the region of point D is an indication of the possible reduction in capacity which may result for the interaction of distortional and lateral buckling.

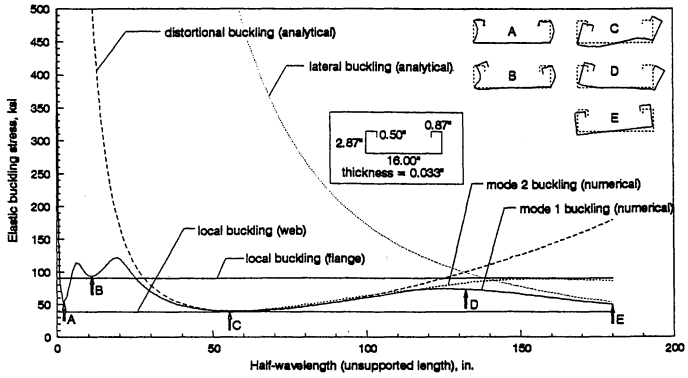

Figure 6 Numerical and analytical buckling curves for the PS-X section

The behavior illustrated by the curves in Figure 7 is more complicated than that for the previous section because of the non-symmetric section configuration. For the non-symmetric section, each leg possesses (in general) different local and distortional buckling behaviors. A comparison of the numerical and analytical curves in Figure 7, shows that:

- *the minimum local buckling stress in the web and flange of the female leg (right leg) are lower that the corresponding minimum local buckling stress defined by the numerical analysis (see point A); not shown, the web and flange local buckling stresses in the male leg are higher than those for the female leg*
- *the analytical distortional buckling stresses in the male leg (region D) are lower than the corresponding stresses from the numerical analysis*
- *the analytical distortional buckling stresses in the female leg (region E) are higher than the corresponding stresses from the numerical analysis*
- *the lateral buckling curves (numerical and analytical) show good agreement*
- *points B and C show that the overall buckling strength of the leg may be significantly decreased by the interaction between local and distortional buckling*

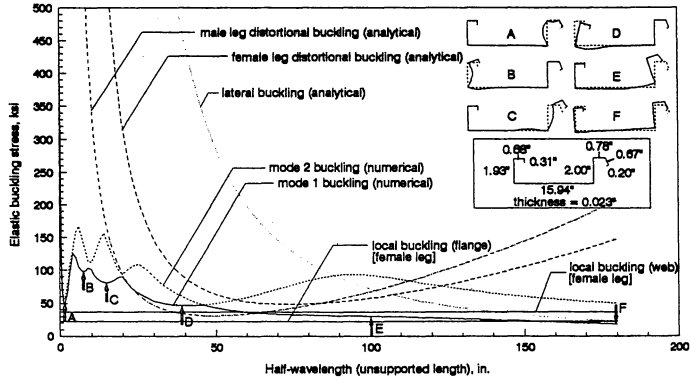

Figure 7 Numerical and analytical buckling curves for the test 1-3 section

Based on analyses of all the buckling curves for the specimens in Douty's and the recent Cornell tests, it appears that in instances where the minimum local buckling stress is lower than the distortional and lateral buckling stresses for a given maximum unsupported length, the locally buckled elements may be capable of developing a significant portion of their post-local buckling strength. On the other hand, if the distortional and lateral buckling stresses are lower than the local buckling stress much of the post-local buckling capacity of the section may not be available. Thus, the magnitude of the distortional buckling stress in comparison to the local buckling stress may be an important consideration in determining the ultimate capacity of a section susceptible to local-distortional buckling interaction.

Unified Design Approach

Peköz (1987) describes the application of an unified approach to the problem of local-lateral buckling interaction. This approach requires the determination of the elastic lateral buckling moment, $M_{cr,lat}$, and the nominal moment, M_n (elastic or inelastic), for the gross section. Using the compressive stress F_n corresponding to the nominal moment, the effective section properties are determined according to the AISI Specification (1986) (the yield stress F_y is replaced by the nominal stress F_n). The ultimate moment, M_u, is then computed as the product of the nominal stress and the effective section modulus, S_e, at that stress.

Since distortional buckling may be regarded as a special case of lateral buckling, the unified approach was used to estimate the capacity of a section subjected to the interaction between local and distortional buckling. Thus, the following design procedure is recommended for estimating the local-distortional buckling interaction strength of a panel:

(1) Assuming the lateral restraints (clips in the actual roof panel system) provide sufficient fixity to prevent lateral displacement, twist, bending and warping, the effective unsupported length of the compression flange, L_e, may be defined as:

$$L_e = k_l L_u \qquad [5]$$

Nethercot and Rockey (1971) suggested that for lateral buckling of doubly symmetric I-beams with fixed ends, k_l may be taken as 0.5. In view of the distortional buckling behavior--lateral deflection of the compression flange--the AISC (1986) recommendation for the effective length factor for fixed-end columns, k_l of 0.65, was assumed to be applicable to this study.

(2) Using equation [1], estimate the elastic distortional buckling moment, $M_{cr,d}$, at L_e. If L_e is greater than the minimum effective unsupported length associated with the minimum elastic distortional buckling stress, the minimum effective length should be used. Compute the elastic buckling stress, $F_{cr,d}$, corresponding to $M_{cr,d}$ as:

$$F_{cr,d} = \frac{M_{cr,d}}{S_g} \qquad [6]$$

where S_g is the gross section modulus for the leg.

(3) Depending on the magnitude of $F_{cr,d}$, determine the nominal compressive stress, F_n, as:

$$F_n = F_{cr,d} : \quad \text{if } F_{cr,d} \le \frac{F_y}{2} \qquad [7a]$$

$$F_n = F_y\left(1 - \frac{F_y}{4F_{cr,d}}\right) : \quad \text{if } F_{cr,d} > \frac{F_y}{2} \qquad [7b]$$

where F_y is the yield strength of the material.

(4) Finally, using the AISI (1986) effective width provisions, determine the effective section modulus, S_e, at F_n and compute the ultimate capacity, M_u, of the section as:

$$M_u = F_n S_e \qquad [8]$$

Using the above design procedure for those specimens in which the test moment (M_t) was less than the ultimate moment due to local buckling only, the ultimate capacities, M_u, of the specimens tested in the Cornell studies were estimated. The predicted ultimate capacities were then compared to the measured test results, M_t, and the comparison is illustrated in Figure 8. For the twenty specimens included in the analysis, the mean and coefficient of variation for the ratio M_t/M_u were 1.074 and 0.136, respectively.

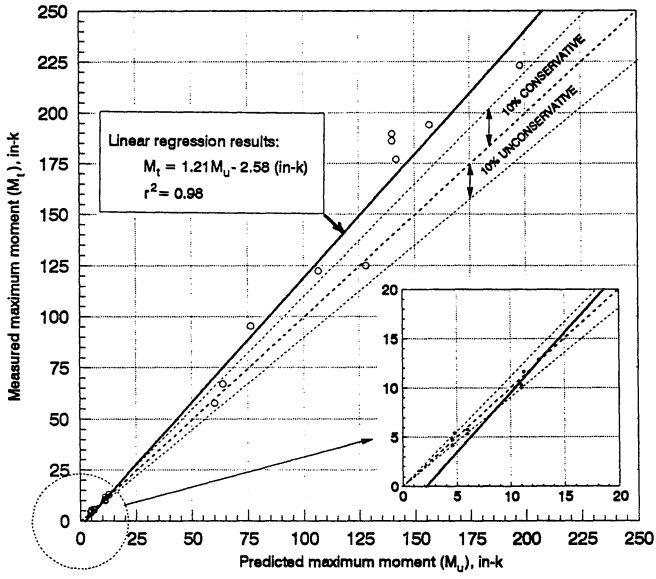

Figure 8 Comparison of measured (M_t) to predicted (M_u) ultimate moment

Comparing the Load and Resistance Factor Design ("LRFD") method with the Allowable Stress Design ("ASD") method, the resistance and safety factor associated with the test statistics were estimated using the following statistical data provided by Hsiao et al. (1988) for cold-formed steel flexural members.

Statistical Variable	Mean	C.O.V.
Material Factor	1.1	0.1
Geometry Factor	1.0	0.1
Dead Load	1.05	0.10
Live Load	1.00	0.25

ratio of the nominal dead to live load, $D_n/L_n = 1/5$
factored load combination = $1.2D_n + 1.6L_n$
reliability index, $\beta_o = 3.0$

The resistance and safety factor associated with the proposed design approach were 0.763 and 2.010, respectively. The AISI Design Manual, Part II (1986), recommends a safety factor of 1.67 for flexural members and 1.92 for column buckling. Since failure due to distortional buckling results from lateral deflection of the compression flange, accompanied by local buckling, it appears prudent that a safety factor of at least 1.92 be applied to panels that may be subject to distortional buckling. Considering the inherent uncertainties in the effective width approach (Cohen, 1987), the proposed design approach appears to be satisfactory.

Conclusion

The behavior of thin-walled panel sections with laterally unsupported compression flanges was studied experimentally, analytically and numerically. A simple analytical expression, consistent with the observed behavior was derived for determining the elastic distortional buckling stress and a design procedure was suggested for the interaction between local and distortional buckling. A comparison of measured and predicted ultimate capacities showed that the design approach gives reasonably accurate results.

Acknowledgements

The work reported in this paper forms part of an ongoing investigation at Cornell University on the behavior of cold-formed steel panels. The project is sponsored by the American Iron and Steel Institute. The support of the American Iron and Steel Institute Task Group and its Chairman, Mr. J. Nunnery, are gratefully acknowledged.

References

AISI Cold-Formed Steel Design Manual, (1986). American Iron and Steel Institute, Washington, DC, August

BFINST6, (1978). Finite Strip Buckling Analysis Program, University of Sydney, Centre for Advanced Structural Engineering, Sydney

Bleich, F., (1952). Buckling Strength of Metal Structures, McGraw Hill, New York, NY, 294-300

Cohen, J. M., (1987). Local Buckling Behavior of Plate Elements, PhD. thesis presented to the Graduate School, Cornell University, August

Douty, R. T, (1962). A Design Approach to the Strength of Laterally Unbraced Compression Flanges, Bulletin No. 37, Cornell University Engineering Experiment Station, April

EC 3 Cold-Formed Steel Sheeting and Members, (1989). Eurocode 3, Appendix A, December

Haussler, R. W., (1964). Strength of Elastically Stabilized Beams, Journal of the Structural Division, ASCE, 90(ST3), June, 219-264

Hsiao, L-E., Yu, W-W., and Galambos, T. V., (1988). AISI LRFD Method for Cold-Formed Steel Structural Members, Ninth International Specialty Conference on Cold-Formed Steel Structures, St. Louis, MO, November, 651-680

Manual of Steel Construction: LRFD (1 ed.), (1986). American Institute of Steel Construction (AISC), Chicago, IL

Nethercot, D. A., and Rockey, K. C., (1971). A Unified Approach to the Elastic Lateral Buckling of Beams, Structural Engineer, Vol. 49, No. 7, July, 321-330

Peköz, T., (1987). Development of a Unified Approach to the Design of Cold-Formed Steel Members, Report CF 87-1, AISI, Washington, DC, March

Specification for Aluminum Structures, Section 1 (1986). Aluminum Association (AA), Washington, DC

Timoshenko, S. P., and Gere, J. M., (1959). Theory of Elastic Stability, McGraw Hill, New York, NY